PERGAMON

Chemical Engineering Science 58 (2003) 1453–1461

Chemical Engineering Science

www.elsevier.com/locate/ces

# Improved processing stability in the hydrogenation of dimethyl maleate to γ-butyrolactone, 1,4-butanediol and tetrahydrofuran

Christoph Ohlinger, Bettina Kraushaar-Czarnetzki*

*Institute of Chemical Process Engineering CVT, University of Karlsruhe, Kaiserstrasse 12, D-76128 Karlsruhe, Germany*

Received 13 June 2002; received in revised form 26 November 2002; accepted 27 November 2002

**Abstract**

In the hydrogenation of dimethyl maleate (DMM) to γ-butyrolactone (GBL), 1,4-butanediol (BDO) and tetrahydrofuran (THF), the performance of the process can be negatively affected by (1) fouling and plugging of the unit through deposition of polymeric by-products and (2) activity drop of the Cu/ZnO-based catalysts through structural changes of the active copper phase at reaction conditions. On the basis of thermodynamic data, we calculated the feed compositions required to prevent condensation of reactants and subsequent formation of polyester deposits in the relevant temperature (453–523 K) and pressure (1–7 MPa) regime. The resulting critical values of the minimum $H_2$/DMM ratios of the feed, when corrected for capillary effects, were found to be in excellent agreement with the limits as experienced in the processing experiments. Conditions for safe and stable gas-phase processing of DMM in a single stage can thus be predicted. The Cu/ZnO-based catalysts were improved by modifying the thermal pre-treatment. As compared to conventional materials of the same composition, they need less runtime to reach stationary performance levels, and their steady state activities are higher. The yield ratio of GBL to BDO can be adjusted through temperature and total pressure because the corresponding hydrogenation attains thermodynamic equilibrium. The subsequent dehydration to THF can be promoted by applying higher temperatures; however, selectivities to tetrahydrofuran remain low over typical Cu/ZnO catalysts unless additional acid sites are implemented.


*Keywords:* Processing; Catalysis; Multiphase reactions; Packed bed; Hydrogenation; Maleic acid anhydride

## 1. Introduction

Growing markets for polybutylene terephthalate, pyrrolidones and polytetramethylene ether glycol are driving the demand for the important chemical intermediates 1,4-butanediol (BDO), γ-butyrolactone (GBL) and tetrahydrofuran (THF) (Morgan, 1997). Moreover, THF and GBL find widespread use as solvents (Weissermel & Arpe, 1997). Today, the major part of these components is still produced via the Reppe process (Reppe & Keyssner, 1941) using acetylene and formaldehyde as the feedstocks. New manufacturing routes, however, will be based on economically more attractive raw materials. Among these, maleic acid anhydride (MAA), which is available from the direct catalytic oxidation of *n*-butane or other linear $C_4$-hydrocarbons with air, will play a dominant role (Morgan, 1997).

MAA as such can be employed and hydrogenated to obtain GBL, BDO and THF. One of the intermediates in the reaction scheme is succinic acid anhydride exhibiting phase transition temperatures (melting point 393 K, boiling point 534 K at $p = 10^5$ Pa), which are considerably higher ($\Delta T \approx 60$ K at atmospheric pressure) than those of MAA. Therefore, MAA is processed in the liquid rather than in the gas phase, using GBL, ethers or alcohols as solvents (Weissermel & Arpe, 1997). Alternatively, dialkyl esters of maleic acid, e.g., dimethyl maleate (DMM) can be used as a feedstock. This route to GBL, BDO and THF requires an additional esterification stage upflow, however, the alcohol can be recovered and recycled, and the reactions can be carried out at mild conditions in the gas phase (Sharif & Turner, 1986). A scheme of the hydrogenation and hydrogenolysis reactions is shown in Fig. 1.

Processing of dialkyl esters in the gas phase would be an attractive option not only because lower pressures are required, but also because well-established fixed-bed reactor technology could be utilised. However, fouling and plugging by polymeric deposits can be a serious problem, in particular, at low temperatures and/or elevated pressures. It is assumed that the polymers are formed upon trans-esterification of dimethyl esters of maleic or succinic acid with the

* Tel.: +49-721-608-3947; fax: +49-721-608-6118.
*E-mail address:* bettina.kraushaar@ciw.uni-karlsruhe.de (B. Kraushaar-Czarnetzki).

0009-2509/03/$ - see front matter © 2003 Elsevier Science Ltd. All rights reserved.
doi:10.1016/S0009-2509(02)00672-3

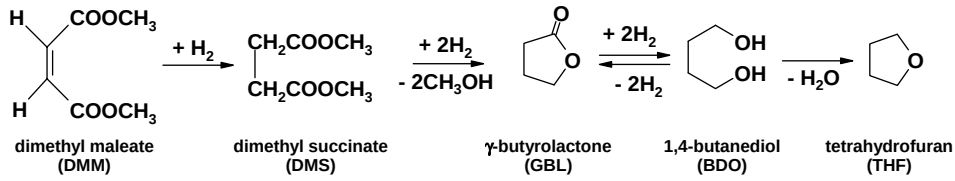


Fig. 1. Reaction scheme for the gas-phase hydrogenolysis of DMM.

product BDO (Kanetaka, Asano, & Masamune, 1970; Schlander & Turek, 1999). Two-stage processes have been proposed in the patent literature, presumably, to circumvent this problem and to maximise the yield of BDO (e.g., Budge, Attig, & Graham, 1993). In the first stage, high temperatures and low pressures can be applied to ensure high conversion of DMM to GBL with little formation of BDO, whereas low temperatures and high pressures in the second stage promote the subsequent formation of BDO and, optionally, of tetrahydrofuran.

Systematic studies addressing the problem of fouling have not been published in the open literature. Rather, most emphasis was given to the screening, selection and characterisation of various catalysts, and many studies focused on reactions of maleic anhydride or esters in the liquid phase. We are particularly interested in the gas phase reaction of DMM in a fixed-bed reactor. In this contribution, we will discuss how polymer formation can be avoided. It will be shown that stable and selective gas phase processing of DMM is possible in a single stage.

We will also address the topic of catalyst stabilisation. The activity of the copper/zinc oxide catalysts, which are mostly applied in this reaction, can be related directly to the copper surface area (Mokhtar, Ohlinger, Schlander, & Turek, 2001). It is a well-known phenomenon, however, that the surface area of copper tends to decrease after exposure to reaction conditions, i.e., hydrogen at elevated pressure and temperature. Not only the drop in activity is a problem, but also the duration of the start of run period before the process is running stationary. Catalysts exhibiting both, a higher initial copper surface and an improved stability against sintering or other structural changes would be desirable. In a recent study, we reported on the preparation and catalytic performance of Cu/ZnO catalysts containing a small amount of alumina, which exhibit higher copper surface areas than the alumina-free materials (Mokhtar et al., 2001). Here, we will show that these $Cu/ZnO/Al_2O_3$ catalysts can be stabilised such that the start of run period is reduced and considerably higher conversion levels can be achieved.

## 2. Experimental

### 2.1. Catalysts

Precipitated $Cu/ZnO/Al_2O_3$ catalysts were prepared with a molar $Al_2O_3$ content of 0.05 and atomic Cu/Zn ratios of 1:2, 1:1 and 2:1 because previous experiments had shown that these compositions result in the highest values of the copper surface areas (Mokhtar et al., 2001). The catalysts were obtained by dropwise mixing of 1 M aqueous $Na_2CO_3$ solution with 1 M solution of copper, zinc and aluminium nitrates under vigorous stirring at 359 K and a constant pH of 7. After cooling down, the precipitates were separated from the mother liquor by filtration, washed several times with deionized water and dried overnight at 353 K. Subsequently, the samples were calcined in air for 3 h at 773 K using a rotary kiln. It should be noted that the calcination temperature applied was chosen much higher than the reaction temperatures required for the hydrogenolysis reaction. The resulting oxide powders were pressed to pellets, crushed and sieved to obtain particle fractions with diameters ranging from 200 to 315 μm.

### 2.2. Catalyst characterisation

The samples were characterised by means of X-ray diffraction (XRD) using Cu-K$\alpha$ radiation. Nitrogen physisorption was carried out to determine the BET surface areas (Micromeritics ASAP 2010). Pore size distributions were measured on a Hg-porosimeter (Autopore III, Micromeritics).

The specific copper surface areas of the catalysts were measured by means of nitrous oxide ($N_2O$) decomposition at atmospheric pressure after reducing the catalyst precursors with hydrogen. The reduction was carried out with 3% $H_2$ in helium at a volumetric flow rate of 300 $cm^3$/min (STP). After raising the temperature from 413 to 513 K at a rate of 20 K/h, the diluted hydrogen stream was replaced stepwise by pure hydrogen within 1 h. Finally, the samples were cooled down to 333 K in pure helium and exposed to a flow of 100 $cm^3$/min (STP) of 0.1% $N_2O$ in helium. The copper surface areas were calculated from the consumed amount of nitrous oxide according to the method described by Chinchen, Hay, Vanderwell, and Waugh (1987).

### 2.3. Processing experiments

Catalytic runs were carried out in a continuous flow unit equipped with a stainless-steel fixed-bed tubular reactor and on-line gas analysis. The packed bed, consisting of catalyst particles diluted with silicon carbide particles of the same size in a volumetric ratio of 1:1, had a diameter of 13 mm and a length of approximately 40 mm. Upflow,

Table 1
Antoine constants of reactants in the hydrogenation of DMM

| Species | Antoine constants | | | Reference |
|---|---|---|---|---|
| | A | B | C | |
| Dimethyl succinate | 10.50956 | 4994.685 | 194.849 | Vogel (1934) |
| γ-Butyrolactone | 11.18937 | 5483.764 | 193.404 | Dykyi, Repas, and Svoboda (1984) |
| 1,4-Butanediol | 8.53422 | 2292.100 | −86.690 | Dykyi and Repas (1979) |
| Tetrahydrofuran | 7.12118 | 1202.942 | −46.818 | Scott (1970) |
| Methanol | 8.15853 | 1569.613 | −34.846 | Ambrose, Sparke, and Townsend (1975) |

the reactor void volume was filled with pure SiC particles in order to ensure a plug flow profile of the feed when contacting the catalyst bed. Prior to the experiments, the catalysts were reduced in situ at atmospheric pressure as described above. Hydrogen and evaporated DMM were fed into the reactor at molar ratios between 45 of 250, hydrogen flow rates varying from 250 to 1000 $cm^3$/min (STP), and total pressures between 1 and 5 MPa. The resulting residence times ($t_{mod}$) were ranging between 1.2 and 13.7 s g/$cm^3$, which is equivalent to space velocities (WHSV) between 0.2 and 2.1 $h^{-1}$. Note that symbols are explained at the end of this article. The reaction temperatures were ranging from 453 to 513 K. On-line analysis was carried out on a Hewlett-Packard 5890 II gas chromatograph equipped with a CP-Wax 52 CB column after pressure release and addition of nitrogen as an internal standard. A more detailed description of the reaction unit has been given elsewhere (Schlander & Turek, 1999).

## 3. Results and discussion

### 3.1. Prevention of fouling

The consequence of fouling is a complete pressure drop in the unit. We observed this phenomenon upon processing at certain combinations of high molar ester fractions in the feed with high pressures and low temperatures. Inspection of the unit after shutdown revealed that a viscous mass had been formed which plugged the catalyst bed and the tubes downflow. Upon cooling down to room temperature, this mass solidifies and turns into a brittle, brownish resin.

The formation of polymeric deposits in the catalyst bed may be promoted or even initiated by the condensation of intermediates and products in the catalyst bed. This assumption was the basis of our considerations. We calculated the minimum dilution with hydrogen required to prevent condensation of intermediates and products at different reaction temperatures and total pressures in the relevant processing range.

Using thermodynamic data from the literature, Antoine constants and vapour pressures of all species involved were determined. The Antoine equation provides a relation between the saturation vapour pressure of pure substances and the temperature

$$\log_{10}\left(\frac{p^*}{1\ \mathrm{Pa}}\right) = A - \left(\frac{B}{T/1K + C}\right). \quad (1)$$

The values of the Antoine coefficients are summarised in Table 1. These data show that the vapour pressures of methanol and tetrahydrofuran are at least one order of magnitude higher than those of the other species within the relevant temperature range. For this reason, further calculations were performed involving dimethyl succinate, BDO and GBL, only. It should be noted that it was not possible to retrieve data for DMM from the public literature. However, it would be a reasonable approximation to use the same data for DMM (atmospheric boiling point: 477.7 K) as for dimethyl succinate (atmospheric boiling point: 473.2 K).

For each component separately, we determined the saturation partial pressure and the molar ratio of hydrogen to DMM in the feed at which the partial pressure of the respective component approaches its saturation partial pressure. The calculations were based on a worst case scenario in so far as the molar fraction of each substance was assumed to be on its maximum value. In the case of the esters, this maximum molar fraction simply represents the value for DMM in the feed. In the case of GBL, total conversion of the dimethyl esters was assumed. The maximum possible molar fraction of BDO was calculated from the equilibrium constant of the hydrogenation of GBL:

$$(CH_2)_3COO + 2H_2 \leftrightarrow HO(CH_2)_4OH.$$

Over the catalysts used, the selectivity for the subsequent dehydration of BDO to THF is low, and the thermodynamic equilibrium in the hydrogenation of GBL is attained already after short residence times. Because hydrogen is always present in large excess, its partial pressure can be approximated with the value of the total pressure, and the equilibrium constant $K_p$ of the hydrogenation can be expressed as

$$K_p = \left(\frac{x_{BDO}}{x_{GBL}}\right)\left(\frac{p^\circ}{p}\right)^2. \quad (2)$$

Equilibrium constants and reaction enthalpies as determined from catalytic experiments were reported recently (Schlander & Turek, 1999). Based on these results, we used values of $K_p = 1.533 \times 10^{-3}$ (at 473 K) and

Table 2
Calculated molar $H_2$/DMM ratios of the feed at which condensation of DMS, GBL and BDO, respectively, may occur. Bold values represent highest values for a $T$, $p$-data pair

| | Dimethyl succinate (DMS) | | | | | | | γ-Butyrolactone (GBL) | | | | | | | 1,4-Butanediol (BDO) | | | | | | |
|---|---|---|---|---|---|---|---|---|---|---|---|---|---|---|---|---|---|---|---|---|---|
| $p$ (MPa) | 1 | 2 | 3 | 4 | 5 | 6 | 7 | 1 | 2 | 3 | 4 | 5 | 6 | 7 | 1 | 2 | 3 | 4 | 5 | 6 | 7 |
| $T$ (K) | Molar $H_2$/DMM ratios of the feed | | | | | | | | | | | | | | | | | | | | |
| 453 | 15 | 31 | 46 | 62 | 78 | 94 | 110 | **16** | 19 | 40 | 62 | 84 | 106 | 127 | 10 | **50** | **105** | **164** | **223** | **281** | **338** |
| 463 | 11 | 23 | 35 | 47 | 59 | 71 | 83 | **13** | 12 | 26 | 43 | 59 | 75 | 91 | 5 | **28** | **63** | **103** | **143** | **183** | **223** |
| 473 | 8 | **18** | 27 | 36 | 45 | 55 | 64 | **10** | 7 | 17 | 29 | 41 | 53 | 66 | 3 | 15 | **38** | **64** | **92** | **120** | **148** |
| 483 | 6 | **13** | 21 | 28 | 35 | 42 | 49 | **8** | 4 | 11 | 19 | 28 | 38 | 47 | 3 | 9 | **22** | **40** | **59** | **79** | **99** |
| 493 | 5 | **10** | **16** | 22 | 27 | 33 | 38 | **6** | 3 | 7 | 13 | 19 | 26 | 34 | 3 | 5 | 13 | **25** | **38** | **52** | **67** |
| 503 | 3 | **8** | **12** | **17** | 21 | 26 | 30 | **5** | 3 | 4 | 8 | 13 | 18 | 24 | 3 | 3 | 8 | 16 | **25** | **35** | **45** |
| 513 | 3 | **6** | **10** | **13** | **17** | 20 | 24 | **4** | 3 | 3 | 6 | 9 | 13 | 17 | 3 | 3 | 5 | 10 | 16 | **23** | **30** |
| 523 | 2 | **5** | **7** | **10** | **13** | **16** | 19 | **3** | 3 | 3 | 4 | 6 | 9 | 12 | 3 | 3 | 3 | 6 | 10 | 15 | **20** |

$\Delta H_r^{\Theta} = -65$ kJ/mol in combination with Eq. (2) and the van't Hoff equation to calculate the maximum attainable molar fraction of BDO in the reaction mixture at relevant total pressures and temperatures.

Table 2 provides the calculated molar $H_2$/ester ratios in the feed at which condensation of dimethyl succinate, GBL or BDO may occur. Bold values indicate which is the highest among the three compound-specific ratios at a given temperature–pressure pair. The data show that condensation of GBL is critical only at a low total pressure. At pressures above 1 MPa, dimethyl succinate and BDO show a higher tendency to condense than GBL. Both these compounds require similar $H_2$/ester ratios in the feed to prevent condensation at medium pressure and temperature. At high pressures ($\geqslant 7$ MPa), however, condensation of BDO is most critical in the whole temperature range, if the feed is not sufficiently diluted with hydrogen. In Fig. 2, we combined the data of the three compounds. The plots allow for the estimation of the minimum molar $H_2$/DMM ratio in the feed which should be adjusted to prevent condensation of one of the reacting species.

It should be noted that capillary action in the pores of the catalyst has not been taken into account upon calculating the limits shown in Fig. 2 because this is a material-specific effect which cannot be generalised. For the catalysts used in this study, the impact of capillary action was estimated using the Kelvin equation in its most simple form, i.e., assuming cylindrical shape of the pores:

$$\frac{p^*}{p(r_c)} = \exp\left(\frac{2\gamma V_m}{RTr_c}\right). \quad (3)$$

According to mercury intrusion measurements, the catalysts exhibited mesopores with a mean pore diameter of $d = 25$ nm. In Eq. (3), the value of the radius of the curvature was varied between $r_c = d = 25$ nm for a wetted pore and $r_c = d/2 = 12.5$ nm for a filled pore. Precise values of the surface tensions ($\gamma$) of the reaction mixture at reaction temperature are not known; however, the range between 0.01 and 0.12 N/m is typical of short-chain diols and water. For

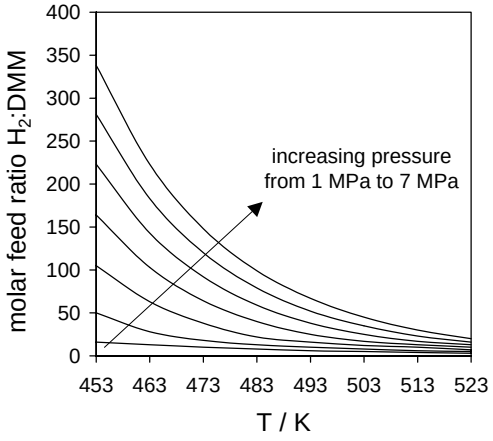


Fig. 2. Minimum molar $H_2$/DMM ratio of the feed required to prevent condensation of a reaction species on a flat interface as a function of the reaction temperature. Curves represent total pressures from 1 to 7 MPa.

the magnitude of $V_m$, the molar volume of 1,4-butanediol ($V_m = 102.41 \times 10^{-6}$ m$^3$/mol) was inserted because this is the most critical component in the reaction mixture at elevated pressure. The resulting drop in vapour pressure and, correspondingly, the shift of the $H_2$/ester limits is most pronounced for the lowest value of $r_c$ and the highest value of $\gamma$.

As an example, Fig. 3 shows the minimum $H_2$/DMM ratio in the feed at a total pressure of 5 MPa calculated for $r_c = d/2 = 12.5$ nm and $\gamma = 0.12$ N/m, representing maximum capillary action in our catalysts at this pressure (dotted line). The comparison with the corresponding results for a flat interface (solid line) shows that the effect of capillaries is pronounced, in particular, at low temperatures. Fig. 3 also contains information about our processing experiments. The open circles indicate experimental conditions where no polymer deposition occurred and complete mass balances were validated. Fouling and complete pressure drop was observed in two experiments (filled circles) at a lower $H_2$/DMM feed

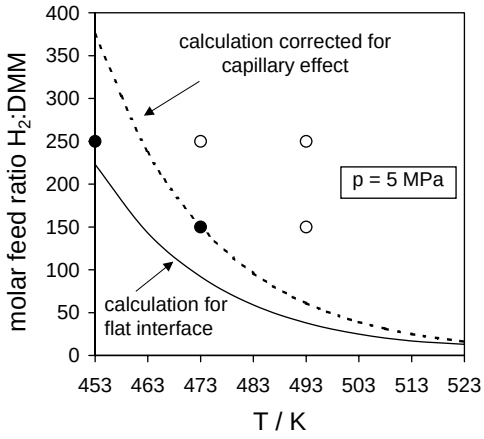


Fig. 3. Minimum molar $H_2$/DMM ratio of the feed required to prevent condensation of a reaction species at 5 MPa on a flat interface (solid line) and in a filled pore with a radius of the meniscus of $d_{pore}/2 = 12.5$ nm (dotted line). Experimental conditions at which fouling and reactor plugging was observed: filled circles; stable processing was possible without fouling: open circles.

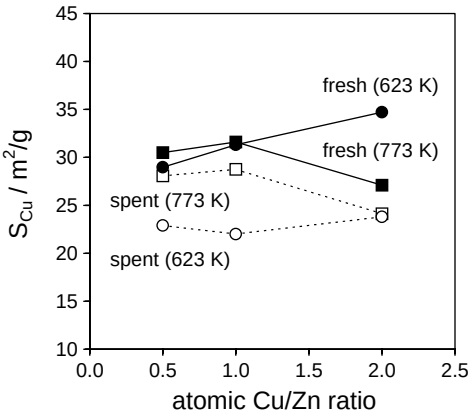


Fig. 4. Copper surface areas of catalysts with different atomic Cu/Zn ratios. Fresh catalysts: closed symbols; spent catalysts: open symbols: Calcination temperature of the precursor 623 K: circles; 773 K: squares.

ratio or temperature, respectively. These critical experimental conditions coincide with those predicted by our calculations.

The perfect agreement between calculated $H_2$/ester limits and those established by experiments should not be overinterpreted because simplifications have been made in the calculations which have opposing effects. A curvature radius of $r_c = d/2$ for a filled rather than for a wetted pore in combination with the highest values of the surface tension ($\gamma$) represents a conservative assumption resulting in a strong increase in the $H_2$/ester limits. On the other hand, the application of Eq. (3), which is applicable only for straight cylindrical pores of equal size, underestimates the capillary effect in a real catalyst pore system. Actually, the narrowest pores, pore mouths and bottle necks rather than the mean mesopore size ($d$) are governing the conditions at which condensation of reactants can start. It may well be that the quantitative impacts of these simplifications are compensating each other to a large extent.

It should also be kept in mind that all calculations were based on the assumption that every species except for THF is present in a maximum molar fraction. This was reasonable in view of the properties of the catalysts used in this study. As will be shown below, these catalysts produce an equilibrium mixture of GBL and BDO and exhibit a low selectivity for THF. The data in Table 2 indicate that BDO has the strongest impact on the $H_2$/DMM ratios required at high pressures. However, catalysts with a high activity in the dehydration of BDO to THF would allow for high-pressure processing at considerably lower $H_2$/ester ratios in the feed than the catalysts used in this study. Thus, the molar $H_2$/DMM limits shown in Figs. 2 and 3 should be considered as a first approximation. To make more accurate predictions about the operational window of stable processing it is mandatory to implement catalyst-specific data concerning the pore size distribution and the selectivity pattern of the reactants involved.

### 3.2. Catalyst stabilisation

The analyses of our catalyst precursors by means of XRD showed that the phase composition depends on the composition of the sample. Hydrozincite and aurichalzite phases are present at low Cu/Zn ratios, whereas malachite is the only crystalline phase at high Cu/Zn ratios. Calcined samples, however, consist only of CuO and ZnO.

While pore size distributions (mean pore diameters around 25–30 nm) and BET surface areas (60 $m^2/g$) of the catalysts were almost identical, copper surface areas were found to depend on the copper content and on the catalyst history. Generally, we observed that spent catalysts exhibit a lower surface area of copper than fresh catalysts. However, the surface loss upon reaction is the less pronounced, the higher the temperature used to calcine the catalyst precursors. On the other hand, calcination temperatures chosen too high result in a low start-of-run value of the copper surface. It was found that a temperature around 773 K represents an optimum for the calcination of our catalyst precursors. This value is 150 K higher than the calcination temperature employed in previous studies (e.g., Mokhtar et al., 2001), and it is 280 K above the highest reaction temperature in the catalytic experiments. A further factor of importance appears to be the temperature distribution in the catalyst bed during calcination. Fig. 4 shows copper surface areas of catalysts with different copper content, obtained by static calcination of the precursors in a muffle oven at 623 K (circles) and by calcination under mixing in a rotary kiln at 773 K (squares), respectively. Comparing the data of fresh and spent samples in Fig. 4 reveals that the loss of copper surface area is only about 8% after high temperature

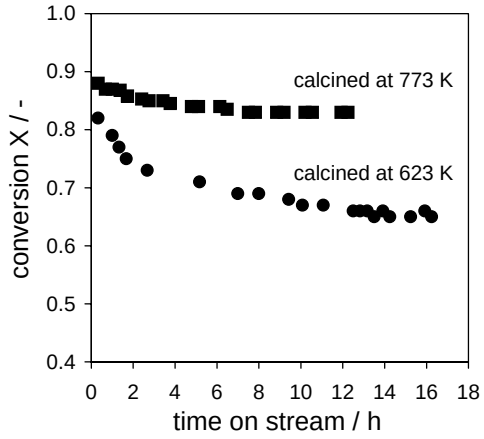


Fig. 5. Conversion of dimethyl succinate with time on stream. Calcination temperature of the precursor 623 K (Cu/Zn = 2 : 1): circles; 773 K (Cu/Zn = 1 : 2): squares. Reaction conditions: $T$ = 513 K; $p$ = 10 bar; molar $H_2$/ester feed ratio = 45.

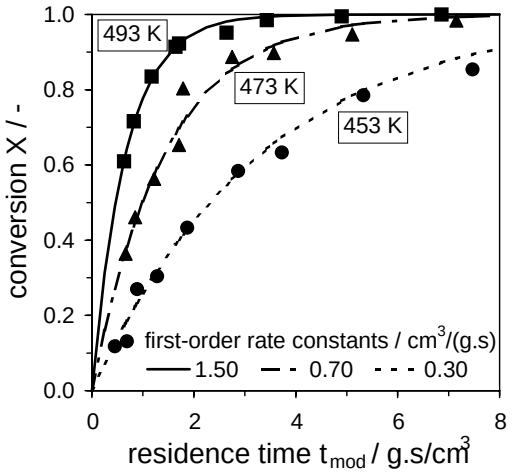


Fig. 6. Conversion of dimethyl succinate as a function of the modified residence time. Reaction temperatures: $T$ = 453 K (circles); 473 K (triangles); 493 K (squares). Catalyst: Cu/Zn = 1 : 1; total pressure: $p$ = 25 bar; $H_2$/ester ratio = 250.

treatment in the rotary kiln whereas it amounts to about 20%, if the precursor was calcined at 623 K and static conditions.

The loss of catalyst activity follows a similar trend. As an example, the initial catalytic performances of two samples are shown in Fig. 5. The filled circles there represent data from the catalyst with the highest initial copper surface area after static calcination at 623 K. This catalyst displays a much stronger deactivation than the catalyst calcined in the rotary kiln at 773 K (filled squares), and it requires about double time to attain its steady state.

Actually, it was our purpose to achieve this latter effect, i.e., the reduction of the initial unsteady-state period by increasing the calcination temperature. It was not expected that catalysts with higher copper surface areas and, consequently, higher activities could be obtained. We assume that the size distribution of the copper particles in these catalysts is more even because calcination in a rotary kiln avoids the occurrence of temperature gradients. If precursor particles of similar size can be produced, it is possible to reduce the effect of Ostwald ripening, i.e., the growth of large Cu particles at cost of small Cu particles under hydrogenation conditions. A more detailed characterisation of the effects of temperature and temperature gradients on the catalyst structure is the subject of current investigations.

### 3.3. Conversion and selectivity

The first step in the reaction scheme, the hydrogenation of DMM to dimethyl succinate, is a very fast reaction. Complete conversion of DMM was observed in all catalytic experiments. Therefore, the conversion of dimethyl succinate to subsequent products was taken as a measure for the catalytic activity. Some exemplary plots of the conversion of dimethyl succinate as a function of the modified residence time are depicted in Fig. 6 for runs at a pressure of 25 bar and a $H_2$/ester ratios in the feed of 250. The symbols represent experimental data obtained during the steady-state processing phase after approximately 8 h on stream. The connecting lines were calculated on the basis of simple first-order kinetics for the conversion of dimethyl succinate according to

$$r = kc_{\mathrm{DMS}} \tag{4}$$

with

$$k = -\ln \frac{(1-X)}{t_{\mathrm{mod}}}. \tag{5}$$

The values of the rate coefficients at 453, 473 and 493 K are given at the bottom of Fig. 5. The detailed kinetic analysis will be reported in the future.

Provided that the $H_2$/ester ratio of the feed is sufficiently high to prevent fouling, the catalysts produce no coke or tar. Unwanted by-products such as 1-butanol or carbon dioxide are formed in negligible traces, only. For this reason and because carbon mass balances were validated (±2%) in our experiments, the reactor (integral) selectivity could be defined on the basis of molar fractions of the $C_4$-products produced from dimethyl succinate

$${}^{R}S_i = \frac{x_{i,\mathrm{C_4}}}{\sum x_{i,\mathrm{C_4}}}. \tag{6}$$

In Fig. 7, reactor selectivities to $C_4$-products at 25 bar pressure and a $H_2$/ester ratio of 250 in the feed are plotted *versus* the dimethyl succinate conversion. It can be seen that higher temperatures favour the production of GBL at cost of BDO. A closer inspection of the data reveals that the molar ratio of BDO to GBL at DMS conversions above 80% is close to the thermodynamic equilibrium ratio which can be calculated with Eq. (2). The magnitude of the constant $K_p$

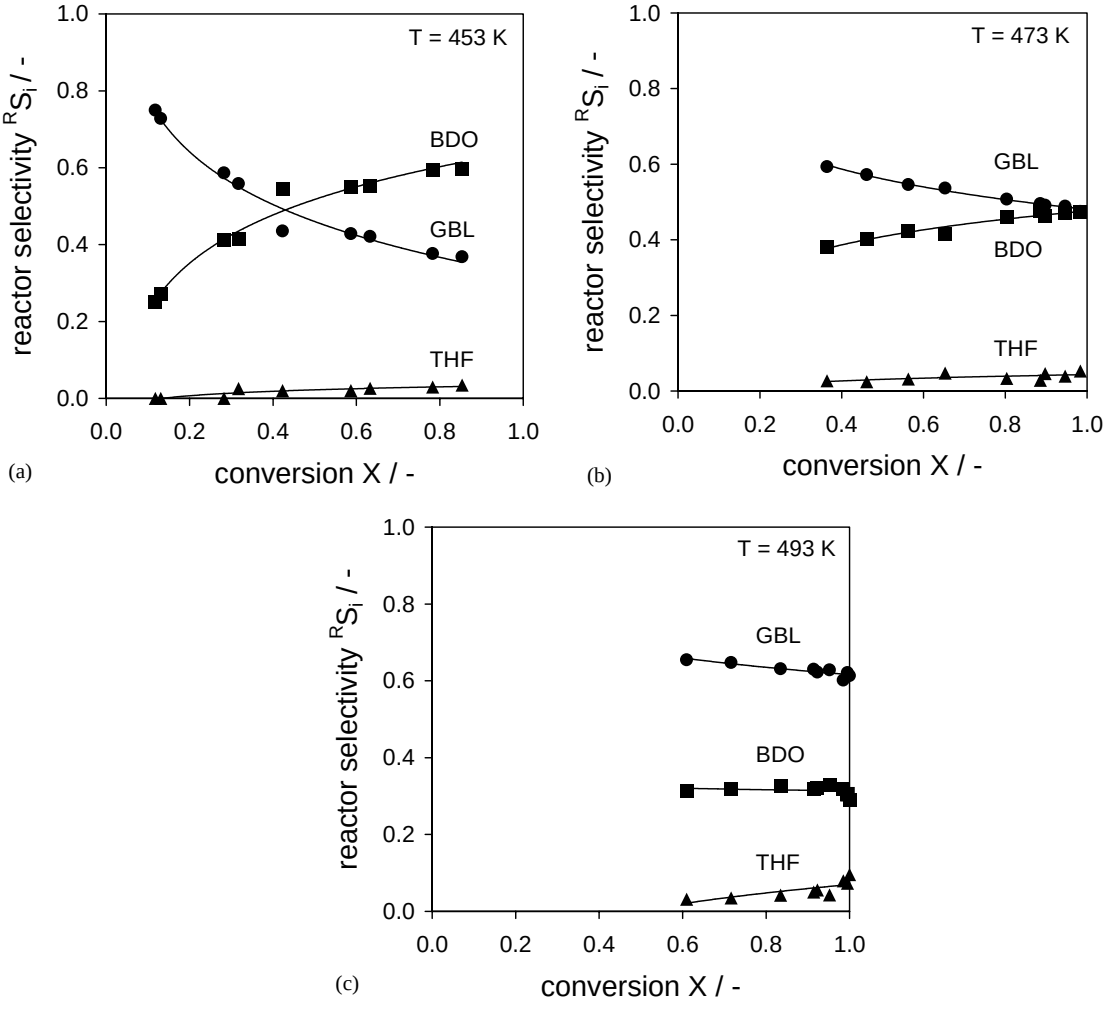


Fig. 7. Selectivities to BDO (squares), GBL (circles) and THF (triangles) versus conversion of dimethyl succinate. Catalyst: Cu/Zn = 1 : 1; total pressure: $p = 25$ bar; $H_2$/ester ratio = 250. Reaction temperatures: 453 K (a), 473 K (b) and 493 K (c).

Table 3
Reactor selectivities of GBL, BDO and THF at a dimethyl succinate conversion of 0.99 over catalyst with Cu/Zn = 1 : 1; $p = 25$ and 50 bar, $T = 493$ K

| | $p = 25$ bar | $p = 50$ bar |
|---|---|---|
| Reactor selectivities at $X = 0.99$ | | |
| GBL | 0.62 | 0.30 |
| BDO | 0.30 | 0.64 |
| THF | 0.07 | 0.06 |
| Experimental selectivity ratio (BDO:GBL) | | |
| | 0.48 | 2.13 |
| Thermodynamic equilibrium ratio (BDO:GBL) | | |
| | 0.49 | 1.96 |

decreases with increasing temperature, and the yield ratio of BDO to GBL increases with pressure. The data in Table 3 confirm that doubling of the pressure (from 25 to 50 bar) results in an increase in the BDO/GBL molar ratio with a factor of approximately 4. The dehydration of BDO to THF is obviously not fast enough to disturb the equilibrium distribution of BDO and GBL.

It should be noticed that low selectivities to THF are a typical feature of catalysts consisting entirely of Cu and ZnO. The catalysts employed in this study also contain a minor amount of $Al_2O_3$ which, however, has no significant effect on the product slate as compared to pure Cu/ZnO catalysts. High reaction temperatures and high residence times promote the dehydration reaction of BDO to THF to some extent, but the possibilities to influence the selectivity to THF *via* adjustment of process conditions are limited. Rather, the nature of the catalyst surface must be altered, e.g., by increasing the number of acid sites to accelerate the BDO dehydration. Recently, we have developed new catalysts with which THF yields of almost 100% can be achieved at reaction conditions comparable to those reported in this article. Because THF exhibits a much higher saturation vapour pressure than the other $C_4$-products, such catalysts should allow for the processing of DMM at lower, i.e.,

economically more attractive $H_2$/DMM ratios in the feed. We will report on this work in the future.

## 4. Conclusions

Two independent problems are typically encountered in the processing of dimethyl maleate to GBL, BDO and THF: (1) the presence of hydrogen at reaction conditions promotes sintering of the active copper surface, resulting in a drop of the catalyst activity after start of run; (2) polymeric deposits, most probably polyesters, can be formed from intermediates and products, causing fouling and plugging of the unit. We have shown that both these problems can be solved.

The formation of polymeric material can be prevented by adjusting the ratio of hydrogen to DMM in the feed to the desired reaction temperature and pressure. We have reported pressure- and temperature-dependent borderlines of minimum $H_2$/DMM ratios which are tracing out in good approximation those areas which enable safe and stable gas-phase processing in one stage. It was demonstrated that predicted and experimentally determined $H_2$/DMM limits are in excellent agreement when specific catalyst properties are implemented into the calculations. In this context, not only the pore size distribution determining the extent of capillary effects is worth mentioning, but also the catalytic activity in the dehydration of BDO to THF because the concentration of BDO in the catalyst bed has a strong impact on the minimum $H_2$/ester ratios required to prevent fouling. Catalysts displaying high selectivities to THF, for instance, will allow for less dilution of the feed with hydrogen. The catalysts used in this study, however, show a low selectivity to THF, while the yield ratio of BDO to GBL is determined by thermodynamic equilibrium and can be adjusted by the choice of reaction temperature and pressure.

The stability of the catalysts was improved by a change in the calcination conditions of the CuO/ZnO/AlO(OH) precursors. The loss of active copper surface area during the first hours on stream could be reduced to less than 10% of the value in the fresh state, compared to 30–35% loss observed in former investigations. The improved catalysts reached a steady performance within shorter processing time, and they displayed higher steady-state activities.

## Notation

| | |
|---|---|
| $A, B, C$ | antoine constants |
| $c_i$ | concentration of species $i$, mol/cm$^3$ |
| $d$ | mean pore diameter, nm |
| $K_p$ | equilibrium constant |
| $k$ | rate coefficient, cm$^3$/(g s) |
| $p$ | pressure, Pa |
| $p^\circ$ | standard pressure, Pa |
| $p^*$ | saturated partial pressure, Pa |
| $r$ | catalyst-mass specific rate of the reaction, mol/(g s) |
| $r_c$ | radius of the curvature, nm |
| $R$ | gas constant, 8.314 J/(mol K) |
| $S_{Cu}$ | copper surface area, m$^2$/g |
| ${}^R S_i$ | reactor selectivity of species $i$ |
| $T$ | temperature, K |
| $t_{mod}$ | modified residence time, g s/cm$^3$; defined as the ratio of the catalyst mass (basis: total mass of the calcined precursor loaded into the reactor) to the total volumetric flow at reaction conditions |
| $V_m$ | molar volume, m$^3$/mol |
| WHSV | weight hourly space velocity, h$^{-1}$; defined as the ratio of the mass flow of dimethyl maleate into the reactor to the catalyst mass (basis: total mass of the calcined precursor loaded into the reactor) |
| $x_i$ | molar fraction of species $i$ |
| $x_{i,C_4}$ | molar fraction of $C_4$ product species $i$ |
| $X$ | conversion of dimethyl succinate |
| $\gamma$ | surface tension, N/m |

*Abbreviations*

| | |
|---|---|
| DMM | dimethyl maleate |
| DMS | dimethyl succinate |
| GBL | $\gamma$-butyrolactone |
| BDO | 1,4-butanediol |
| MAA | maleic acid anhydride |
| THF | tetrahydrofuran |

## References


Ambrose, D., Sprake, C. H. S., & Townsend, R. (1975). Thermodynamic properties of organicoxygen compounds. XXXVII. Vapour pressures of methanol, ethanol, pentan-1-ol, and octan-1-ol from the normal boiling temperature to the critical temperature. *Journal of Chemical Thermodynamics*, *7*, 185–190.

Budge, J. R., Attig, T. G., & Graham, A. M. (1993). Two-stage maleic anhydride to tetrahydrofuran and gammabutyrolactone. *U.S. Patent* 5.196.602.

Chinchen, G. C., Hay, C. M., Vanderwell, H. D., & Waugh, K. C. (1987). The measurement of copper surface areas by reactive frontal chromatography. *Journal of Catalysis*, *103*, 79–86.

Dykyi, J., & Repas, M. (1979). *The vapor pressure of organic compounds*. Bratislava: Slovakian Academy of Science.

Dykyi, J., Repas, M., & Svoboda, J. (1984). *The vapor pressure of organic compound*, *Part* 2. Bratislava: Slovakian Academy of Science.

Kanetaka, J., Asano, T., & Masamune, S. (1970). New process for production of tetrahydrofuran. *Industrial Engineering Chemistry*, *62*, 24–32.

Mokhtar, M., Ohlinger, C., Schlander, J. H., & Turek, T. (2001). Hydrogenolysis of dimethyl maleate on Cu/ZnO/$Al_2O_3$ catalysts. *Chemical Engineering Technology*, *24*, 423–426.

Morgan, M. L. (1997). The rapidly changing world of 1,4-butanediol. *Chemistry and Industry*, *3*, 166–168.

Reppe, W., & Keyssner, E. (1941). Production of alkinols. *US Patent* 2.232.867.

Schlander, J. H., & Turek, T. (1999). Gas phase hydrogenolysis of dimethyl maleate to 1,4-butanediol and $\gamma$-butyrolactone over

copper/zinc oxide catalysts. *Industrial Engineering Chemical Research*, *38*, 1264–1270.

Scott, D. W. (1970). Tetrahydrofuran: Vibrational assignment, chemical thermodynamic properties, and vapor pressure. *Journal of Chemical Thermodynamics*, *2*(6), 833–837.

Sharif, M., & Turner, K. (1986). *US Patent* 4.584.419.

Vogel, A. I. (1934). Physical properties and chemical constitution. I. Ester of normal dibasic acids and substituted malonic acids. *Journal of Chemical Society* 333–341.

Weissermel, K., & Arpe, H.-J. (1997). *Industrial organic chemistry* (3rd ed.). Weinheim, Germany: Wiley VCH.